Structural Characterization of Separated H DNA Conformers†

J. N. Mark Glover, Chuck S. Farah, and David E. Pulleyblank*
Department of Biochemistry, University of Toronto, Toronto, Ontario M5S 1A8, Canada
Received June 20, 1990; Revised Manuscript Received August 23, 1990

ABSTRACT: Polypyrimidine/polypurine DNA sequences in plasmids can adopt protonated triplex-containing structures (H DNA) in response to negative superhelical stress and low pH. A $d(TC)_{17}$-$d(GA)_{17}$ insert adopts two isomeric protonated structures, which differ in degree of helical unwinding. The variant forms of individual topoisomers were separated by agarose gel electrophoresis and their reactivities to permanganate and acid-induced depurination were compared. Depurination patterns of the individual conformers indicate that in the more mobile form (H-y5) the 5′-half of the $d(GA)_n$ strand participates in a triplex while in the other (H-y3) the 3′-half forms the triplex. The H-y5 form is more stable than the H-y3 form at low negative superhelix densities. Because of the difference in helical unwinding, the H-y5 form becomes relatively less stable as the superhelix density increases. Topological models of the two forms show that providing there is no linkage at the tips of the triple helical segments one more positive twist is localized in the H-y5 form than in the H-y3 form. The foldback in the pyrimidine strand of the H-y5 form is less accessible to solvent than that of the H-y3 form as assessed by its lower reactivity to permanganate. Consideration of a pyrimidine loop model (Harvey, S. C., Luo, J., & Lavery, R. (1988) *Nucleic Acids Res. 16*, 11795–11809) suggests that the unique stability of the H-y5 form results from Watson–Crick base pairs between residues of the $d(TC)_n$ loop and the $d(GA)_n$ strand as it exits the triplex.

The polypyrimidine/polypurine DNA element $d(TC)_n$-$d(GA)_n$ is a common repetitive sequence found intimately associated with transcriptional regulatory elements, recombinational hot spots, and origins of DNA replication thoughout the eukaryotic kingdom [for a review, see Wells et al. (1988)]. Electrophoretic anomalies of supercoiled plasmids that contain these sequences as well as the chemical and nuclease reactivities of the sequences themselves have established that they can adopt protonated underwound conformations (Lyamichev et al., 1985; Pulleyblank et al., 1985; Hanvey et al., 1988a; Htun & Dahlberg, 1988, 1989; Johnston, 1988; Voloshin et al., 1988). One of two models proposed for the protonated structure of $d(TC)_n$-$d(GA)_n$ is a protonated duplex structure containing Hoogsteen base pairs between cytosine residues protonated at their N3 atoms and guanine residues (Pulleyblank et al., 1985, 1988). In this model S1 nuclease sensitivity was attributed to alterations in the sugar–phosphate backbone torsion angles necessary to accommodate Hoogsteen pairs in a double helix that also contained Watson–Crick pairs. In a second model (H DNA, Figure 1; Lee et al., 1984; Lyamichev et al., 1986) a triplex forms by folding the tract at its center so that the polypyrimidine strand from one half becomes hydrogen bonded to the purine strand of the other via Hoogsteen base pairs. The half of the $d(GA)_n$ strand not involved in the triplex is unpaired. Polypurine/polypyrimidine polymers have previously been shown to form triplexes (Arnott & Selsing, 1974) where the Hoogsteen G-C pairs are protonated (Morgan & Wells, 1968; Lee et al., 1979).

The effects of point mutations on the energies or structures of the protonated states of a variety of polypurine/polypyrimidine tracts were consistent with the H model. Mutations in a complex sequence predicted to disrupt a base triad in an H structure increased the energy cost of the transition while compensatory mutations predicted to restore canonical T·A·T or $C{\cdot}G{\cdot}C^+$ triads restored the low energy of the protonated structure (Mirkin et al., 1987). In simpler polypurine/polypyrimidine sequences, point mutations were found to cause excess chemical reactivity when protonated both at the site of mutation and at sites predicted to be associated with the mutated site in a folded H form (Hanvey et al., 1988b).

The H model predicts that the unpaired half of the $d(GA)_n$ strand and the unpaired polypyrimidine hairpin should be hypersensitive to chemical reagents that react more readily with unstacked DNA than with B DNA. Although the results of some studies are consistent with these predictions (see references cited above), a number of examples of more complex chemical reactivity patterns have been observed that cannot be simply accommodated within the H model (Pulleyblank et al., 1985; Evans & Efstratiadis, 1986; Glover & Pulleyblank, 1990). Two-dimensional gel electrophoresis experiments have shown that single $d(TC)_n$-$d(GA)_n$ elements may adopt a number of different protonated forms, which differ in the extent of helical unwinding resulting from the transition (Pulleyblank, 1988; Htun & Dahlberg, 1989). It has been suggested that two of these structures may correspond to the two distinct H forms: one in which the 5′-half of the pyrimidine strand is Hoogsteen paired to the 5′-half of the purine strand in the triplex (H-y5) and the other in which the 3′-half of the pyrimidine strand is Hoogsteen paired to the 3′-half of the purine strand in the triplex (H-y3) (Htun & Dahlberg, 1989). Folding and strand disproportionation has also been proposed to explain two different non-B states in $d(G)_n$-$d(C)_n$ tracts (Kohwi & Kohwi-Shigematsu, 1988).

In previous studies the presence of variable amounts of different conformational forms in samples being analyzed by chemical probes may have complicated interpretation of the results. Here the reactivity patterns of two isomeric forms adopted by a short $d(TC)_n$-$d(GA)_n$ tract to permanganate and acid-induced depurination have been individually analyzed and are shown to be consistent with the isomeric forms being the H-y5 and H-y3 forms.

Experimental Procedures

DNA. The construction of plasmids pGA34 and pGA_CT

† This work was funded by an operating grant from the Medical Research Council of Canada. J.N.M.G. is a recipient of a Medical Research Council of Canada Studentship.

0006-2960/90/0429-11110$02.50/0

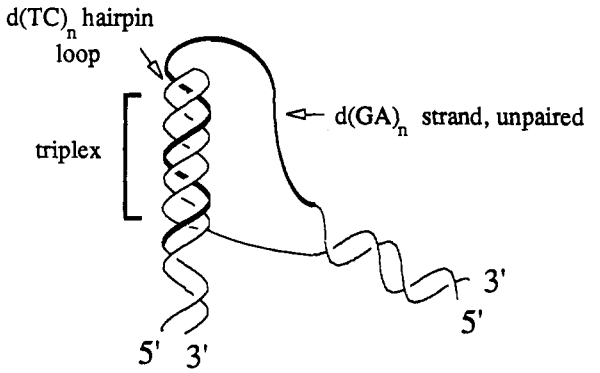

FIGURE 1: Elements of the H DNA structure that allow its detection by chemicals that react with bases. In the illustration the 5'-half of the $d(CT)_n$ strand Hoogsteen pairs with the 5'-half of the $d(GA)_n$ strand to form the triplex [H-y5 form from Htun and Dahlberg (1989)].

been described previously (Glover & Pulleyblank, 1990). Synthetic oligonucleotides were synthesized by using standard (β-cyanoethyl)phosphoramidite chemistry on a Milligen Cyclone DNA synthesizer.

Acid-Induced Depurination. DNA samples were exposed at 23 °C to pH 4.4 buffer for 90–105 h during electrophoresis. No more than one apurinic site was generated per 200 base pairs. Plasmid samples were cleaved with *Bst*EII and directionally 3'-end-labeled adjacent to the $d(GA)_{17}$ tract with reverse transcriptase in the presence of [α-^{32}P]-dATP, dGTP, and dTTP. Strand scission was effected at apurinic sites by treatment of the end-labeled DNA with 10% (v/v) piperidine (90 °C, 15-min reaction time). Sites of depurination were detected by autoradiography after separation of the products on 7% denaturing polyacrylamide gels.

The sites of depurination in the native samples were compared with the depurination patterns in the same sequences under strongly acidic denaturing conditions (10 mM HNO_3, 37 °C, 15-min reaction time).

Construction and Purification of Intermolecular Triplexes (Figure 2). One microgram of an *Hha*I digest of pGA_CT that has a $d(AG)_8$-dA-$d(CT)_8$ insert was mixed in a pH 4.4 buffer (20 mM Tris–acetate, 2.5 mM sodium acetate, 1 mM magnesium acetate, 27.4 mM acetic acid) with 0.035 μg of $d(TC)_8$ (10:1 oligonucleotide/restriction fragment molar ratio). A control sample of the *Hha*I digest was incubated in the pH 4.4 buffer in the absence of the oligonucleotide. The oligonucleotide/fragment and control sample mixtures were incubated for 5 h at 37 °C and electrophoresed on an 18% nondenaturing polyacrylamide gel (4 V/cm, 90 h in the pH 4.4 buffer, left panel, Figure 2). After electrophoresis the bands containing the free insert and the intermolecular triplex were electroeluted from the gel.

Detection of Chemically Modified Sites in Protonated Conformers of pGA34. Fifty micrograms of a mix of pGA34 topoisomers centered at topoisomer -7 was generated by topoisomerase I relaxation in the presence of ethidium bromide (2.4 μg of ethidium/50 μg of pGA34 in 850-μL reaction volume). The topoisomers were separated by preparative electrophoresis in a 1.5% agarose gel in a pH 8.5 buffer (40 mM Tris–acetate, 5 mM sodium acetate, 1 mM EDTA) at 2 V/cm for 24 h. Single topoisomers were electroeluted and checked for purity by electrophoresis at pH 8.5 on a 1.5% agarose gel (left panel, Figure 3A). Purified topoisomers were equilibrated in a 100 mM sodium citrate, pH 4.4, buffer for 1–2 h at 23 °C and subsequently electrophoresed in the pH 4.4 buffer at 0.88 V/cm in a 1.5% agarose gel for 87 h. The gel was stained with ethidium and the DNA recovered from the gel by adsorption to glass from sodium iodide solution (GENECLEAN, BIO 101 Inc.). Sites of depurination in the separated protonated conformers were determined as described above.

To assay permanganate reactivity, approximately 5 μg of each purified topoisomer equilibrated in the pH 4.4 buffer was allowed to react with permanganate (50 μM $KMnO_4$ in a 25-μL reaction volume, 5-min reaction time). The reaction was terminated by addition of NaI (170 μM final concentration). Modified topoisomers were electrophoresed on a 1.5% agarose pH 4.4 gel to separate the protonated conformers as described above. Although modification causes slight broadening of the bands, the isomeric forms of each topoisomer remain stable. Sites of permanganate reaction were detected as described above for depurinated samples except that pGA34 was 3'-end-labeled at the *Xba*I site within the polylinker to analyze the $d(CT)_{17}$ strand. Densitometry (LKB scanning laser densitometer) of autoradiographs of the resulting gels was performed. Integrated densities were normalized with respect to total loading to determine relative rates of depurination or permanganate oxidation.

RESULTS

Acid-Catalyzed Depurination as a Probe of Protonated DNA Conformation. Plasmid DNA incubated for 96 h at pH 4.4 exhibit piperidine-labile sites that result from acid-catalyzed depurination (not shown). To determine whether depurination could be used to demarcate triplexes, the susceptibility to depurination of an intermolecular triplex was compared to that of a control duplex (Figure 2). The intermolecular triplex was formed at pH 4.4 by mixing a $d(CT)_8$ oligonucleotide with a pGA_CT restriction fragment that contained a short $d(GA)_8$-$d(CT)_8$ segment. The short $d(TC)_8$ tracts in pGA_CT can be kinetically trapped in B form at pH 4.4 (Glover & Pulleyblank, 1990), and thus this plasmid was used to compare the depurination patterns of the polypurine tracts in the duplex and triplex forms. The retarded complex containing the $d(GA)_8$-$d(CT)_8$ intermolecular triplex was separated from the free restriction fragments by slow (90 h) nondenaturing polyacrylamide gel electrophoresis at pH 4.4 (left panel, Figure 2). Sites of depurination that developed during the electrophoresis in the purified free and triplex-containing fragments are shown in the right panel of Figure 2. Triplex formation results in a dramatic suppression of depurination within the triplex.

Depurination/Permanganate Reactivities of Two pGA34 Conformers. Previous studies of the chemical reactivities of the protonated $d(TC)_{17}$-$d(GA)_{17}$ tract in pGA34 have revealed changes in reactivity profiles that depend on the level of negative supercoiling (Glover & Pulleyblank, 1990). Two-dimensional gel electrophoresis of pGA34 topoisomers indicates that the $d(TC)_{17}$-$d(GA)_{17}$ insert can adopt two underwound protonated conformations. The more underwound form releases approximately 3.6 superhelical turns, while the less underwound form releases approxiately 2.6 turns (data not shown).

To analyze the structures of the individual conformers, the acid-catalyzed depurination events in the two isomeric conformations that accumulated as the two forms separated on a pH 4.4 gel were determined (Figure 3). Single pGA34 topoisomers were gel purified at pH 8.5 where the $d(TC)_{17}$-$d(GA)_{17}$ insert is not protonated (Experimental Procedures and left panel of Figure 3A). The purified topoisomers were then electrophoresed on a second pH 4.4 agarose gel. Each topoisomer migrated as two bands corresponding to the

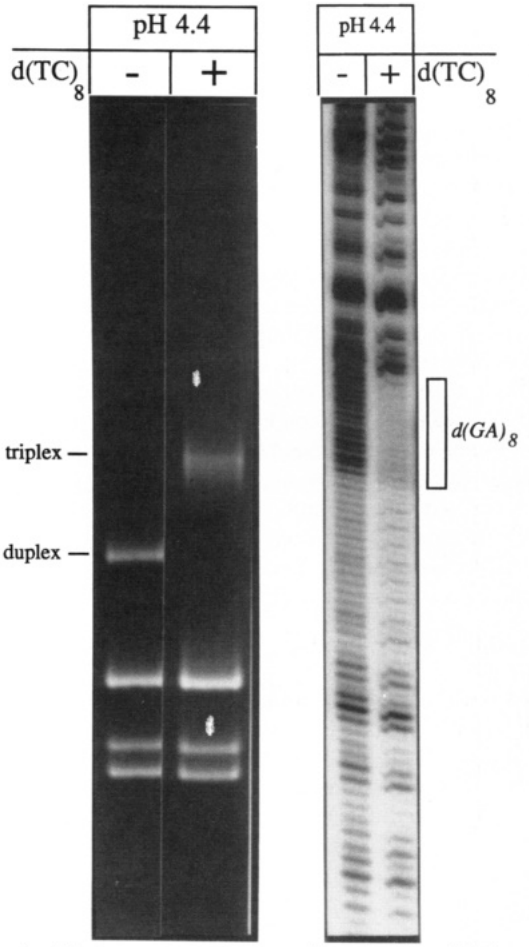

FIGURE 2: Triplexes are resistant to depurination. Right panel: Nondenaturing PAGE of a pGA_CT restriction digest at pH .4.4 in the absence or presence of a $d(TC)_8$ oligonucleotide (see Experimental Proceedures). The positions of the fragment containing the free $d(GA)_8$-$d(CT)_8$ insert (duplex) and of the fragment complexed to $d(TC)_8$ (triplex) are indicated. Left panel: The depurination patterns of the purified free and triplex-containing forms of the restriction fragment (see Experimental Procedures). The $d(GA)_8$ tract that is protected against depurination in the triplex is indicated by a box.

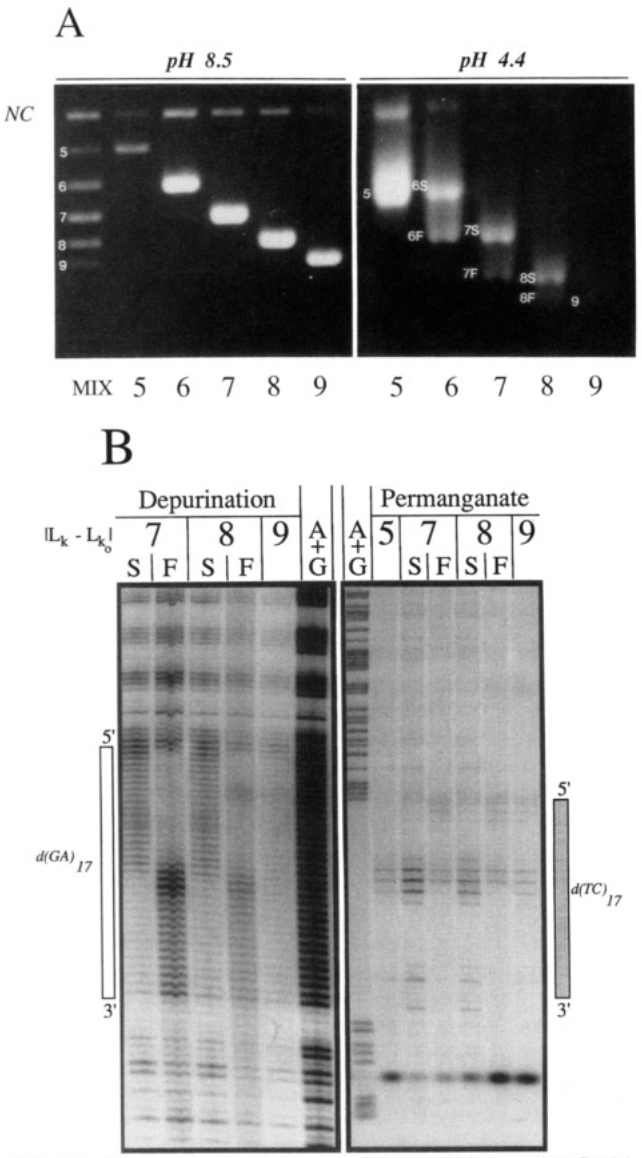

FIGURE 3: Structural characterization of the two H isomers in pGA34. (A) Purification of protonated conformers of pGA34. Left panel: Single topoisomers purified from a mix (left-most lane) electrophoresed at pH 8.5. Right panel: Purified topoisomers run on a pH 4.4 gel adopt two conformations. The $|Lk - Lk_0|$ values [equivalent to $(\alpha - \alpha_0)$ defined by Haniford and Pulleyblank (1983)] are indicated next to each topoisomer. Each topoisomer that contains enough superhelical free energy to undergo a transition splits into two forms: a slow-migrating form (S) and a fast-migrating form (F). "NC" indicates the band corresponding to nicked plasmid. Generation of topoisomers and electrophoresis conditions are described under Experimental Procedures. (B) Left panel: Depurination patterns of the strand containing the polypurine segment in the various protonated forms. Right panel: The permanganate reactivities of the separated forms (see Experimental Procedures). The $|Lk - Lk_0|$ values and the mobility (S or F) for the various species are indicated. "A + G" is a purine ladder.

two protonated forms (right panel, Figure 3A). The patterns of acid-induced depurination in the $d(GA)_n$ strand of these purified forms are shown in the left panel of Figure 3B and the relative rates of reactivity of the individual purines, quantitated by densitometric scans of the autoradiograph, are displayed in Figure 4. Each form has a distinct region corresponding to approximately half of the protonated $d(GA)_n$ tract, which is protected against acid depurination. These protected regions are consistent with both forms containing triplexes. The 3′-half of the purine strand contributes to the triplex of the more underwound, slow mobility form while the 5′-half of the purine strand contributes to the triplex of the faster migrating species. Observations of changes in chemical reactivity with altered superhelix density had previously suggested that these forms correspond to the same two H DNA isomers (Htun & Dahlberg, 1989).

To analyze the structures of the $d(TC)_n$ hairpins of the two forms, purified single topoisomers were allowed to react with permanganate in the pH 4.4 electrophoresis buffer after the transition had been allowed to occur. The oxidized forms were then purified electrophoretically and, after end-labeling, the oxidized residues were cleaved by piperidine treatment. Permanganate oxidizes the C5–C6 double bond of thymines to the piperidine-labile, 5-hydroxy, 6-keto derivative at this pH (Iida & Hayatsu, 1970), a reaction that is sterically inhibited by stacking interactions in B DNA (Glover et al., 1988). The region of the $d(TC)_n$ strand expected to form the hairpin at the tip of the triplex is sensitive to permanganate oxidation in both protonated conformers, suggesting that in both structures pyrimidine bases are unstacked to make the hairpin loop (right panel, Figure 3B). The densitometric analyses shown in Figure 4 reveal quantitative differences in the reaction rates of loop residues in the two forms. In the slow (S) mobility conformer five bases are reactive whereas only three are reactive in the fast (F) mobility conformer. In

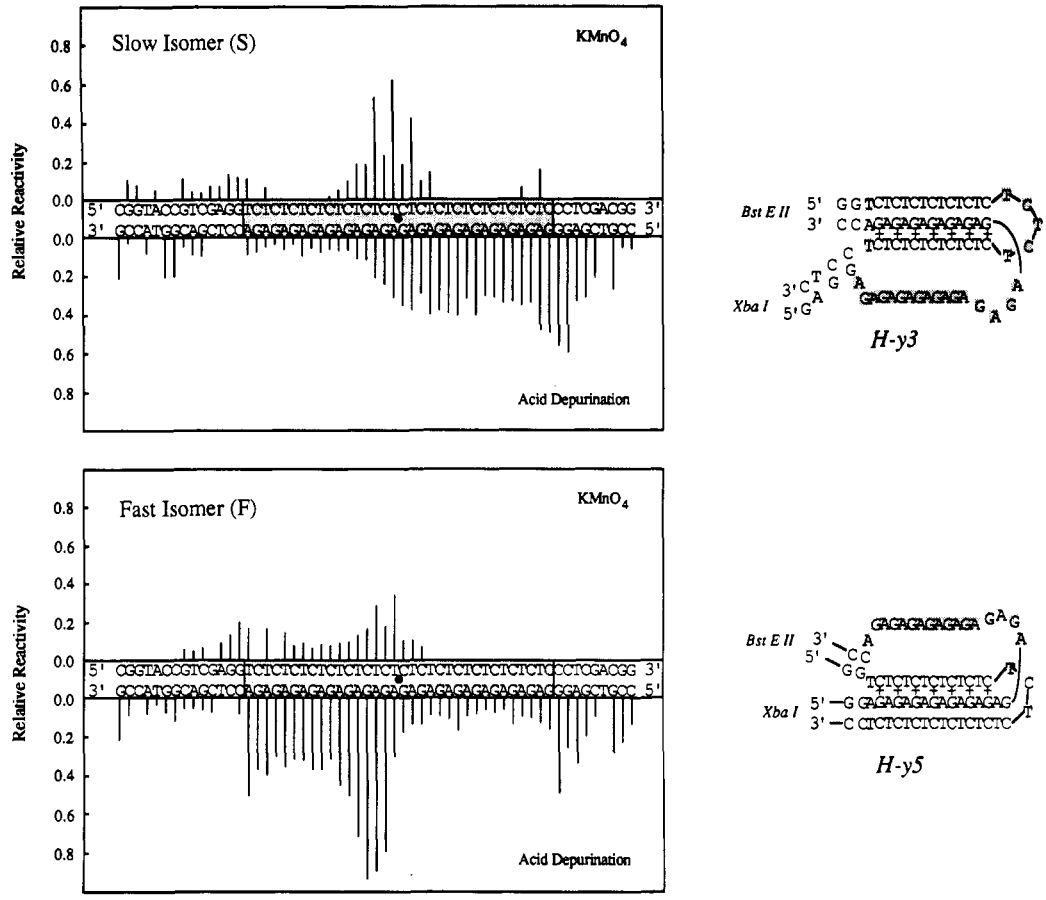

FIGURE 4: Quantitation of the rates of acid-induced depurination and permanganate reactivity in the protonated conformers. Relative reactivities were determined by scanning laser densitometry of the lanes in Figure 3B which display the chemical reactivities of the slow and fast forms of the topoisomer in which $|Lk - Lk_0|$ equals 7. H DNA models that best fit the data are shown. Shaded regions indicate residues hyperreactive to depurination (A's and G's) or permanganate (T's and C's).

addition to the more extended reactive region in the "S" loop, individual residues are approximately twice as reactive as the corresponding residues of the "F" loop.

Discussion

Base protonation labilizes the glycosidic bond at purine DNA residues leading to acid-induced depurination (Zoltewicz et al., 1970; Shapiro & Danzig, 1972). The step determining conformational specificity may be either the protonation step or breakage of the glycosidic bond. Part of the delocalized charge in the protonated G·C Hoogsteen pairs of triplexes may be carried by the guanine base. Since the normal pK_a of deoxyguanosine is ~2.3 (Izatt et al., 1971), the effective degree of protonation of guanine in B DNA at pH 4.4 is ~1%. The observed protection of guanine residues in triplexes against depurination is therefore more likely to result from the greater rigidity of the triplex relative to the B form than from reduction in the average charge on the base. The protection of adenine residues may also be due to triplex inflexibility rather than to inhibition of adenine protonation in the triplex since the N3 atom of adenine, the site most likely to be involved in adenine base depurination, is exposed in both B DNA and the triplex. Residue rigidity may inhibit adoption of a planar transition state at the C1′ atom of purine nucleotide residues. The recently reported inhibition of UV-induced pyrimidine dimer formation in triplexes may also result from reduced conformational flexibility of triplexes relative to the B form since some realignment of adjacent pyrimidine residues is necessary for dimer formation (Lyamichev et al., 1990).

The depurination reactivities measured here define the regions of the purine strands involved in the formation of triplexes in the two isomeric structures formed by the d-$(TC)_{17}$-d$(GA)_{17}$ tract of pGA34 (Figure 4). These data directly identify the more underwound form as the "H-y3" structure, and the less underwound form as the "H-y5" structure in the nomenclature of Htun and Dahlberg and are in agreement with the results of those authors (Htun & Dahlberg, 1989).

Models of oligo$(dT)_n$ hairpins built to conform to the geometrical constraints at the ends of a triplex suggest that the lowest energy five-residue hairpin loop contains four thymines stacked on the 3′-side of the loop and a single unstacked thymine bridging the gap between the single-stranded stack and the triplex (Harvey et al., 1988). Both physical and model studies suggest that the unpaired bases in both A- and B-form DNA and RNA hairpins display simiar stacking patterns (Haasnoot et al., 1986; Blommers et al., 1989, and references cited therein). The five-residue model for the triplex loop (Harvey et al., 1988) is compatible with the observed five reactive pyrimidines in the H-y3 loop but is less consistent with the observed reactivity of three residues in the H-y5 loop. The H models presented in Figure 4 contain triplexes defined by regions protected against depurination. The regions of triplex define which pyrimidine residues form the hairpin loop. The five residues in the H-y3 loop, as well as the hyperreactivity of these residues to permanganate oxidation, agrees with the model of Harvey et al. (1988). However, the five pyrimidines predicted to form the H-y5 loop are not all reactive to permangante. Differences in depurination rates are also observed between the two forms at the centers of the d$(GA)_{17}$ tracts predicted to be opposite the pyrimidine hairpin loops. These differences suggest that interactions between the d$(GA)_n$ strand

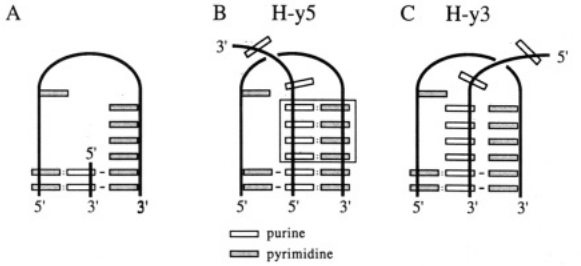

FIGURE 5: Watson–Crick pairs may form between the $d(GA)_n$ strand and the $d(TC)_n$ loop in the H-y5 isomer but not in the H-y3 isomer. (A) A schematic diagram of the 514 loop model (Harvey et al., 1988). (B) Since the $d(GA)_n$ strand exits the loop antiparallel to the pyrimidine stack in the H-y5 isomer, Watson–Crick pairs may be formed in the loop. (C) In the H-y3 isomer, the purine strand is parallel to the pyrimidine stack and thus Watson–Crick pairs cannot form.

and the H-y5 pyrimidine hairpin partially protected the hairpin against permanganate reaction and that equivalent interactions do not occur in the H-y3 form. We propose that the interaction occurs through Watson–Crick base pairs formed between pyrimidine residues stacked on the 3′-side of the hairpin and the antiparallel $d(GA)_n$ strand as it exits the triplex at the hairpin (Figure 5). An equivalent interaction cannot occur in the H-y3 structure since here the $d(GA)_n$ strand must lie parallel to any 3′-stack in the pyrimidine hairpin. The additional stabilization obtained through these interactions in the H-y5 hairpin loop may contribute to the greater apparent stability of this form relative to the H-y3 form at low superhelix densities (Htun & Dahlberg, 1989; Glover & Pulleyblank, 1990). Htun and Dahlberg (1989) previously suggested that the preference for the H-y5 form under these conditions may be a kinetic consequence of the different geometries of the transition states to the two forms. Due to the difficulty in determining whether true thermodynamic equilibrium between Hy-3 and Hy-5 isomers has been attained, the question of whether the H-y5 form is kinetically or thermodynamically favored over the H-y3 form at low superhelix densities remains unresolved.

An intrinsic topological inequality distinguishes H-y3 and H-y5 isomers with unlinked foldback loops equivalent to those illustrated in Figure 6. A difference in the helical twist of the two structures arises from the directionality of the third strand, which imposes overall direction on the triplex. In consequence, the complementary strands must cross each other once more in the H-y5 form than in the H-y3 form. The H-y5 and H-y3 pair of structures illustrated in Figure 6A have one turn of the triplex and a positive (right handed, antiparallel) half twist not contained within the H structure. Unwrapping the polypyrimidine hairpin from the polypurine strand in the triplex reveals that in the H-y5-containing structure the strands are topologically linked ($L_k = +1$, right-most structure in Figure 6A). Unwrapping the polypyrimidine hairpin of the H-y3 structure shows that here the strands are unlinked ($L_k = 0$). The H-y5 structure therefore traps one more positive twist and releases one less negative superhelical turn than the H-y3 form (as observed here for pGA34, Figure 3A). Htun and Dahlberg (1989, 1990) arrived at an equivalent conclusion by considering untwisting involved in the prenucleation of the two H DNA forms.

There is an interesting topological consequence of a strand cross at the tip of an extruded H triplex. As illustrated in Figure 6B this reverses the unwinding relationship between H-y5 and H-y3 forms making the H-y5 structure the more underwound. Longer $d(TC)_n$-$d(GA)_n$ tracts than that of pGA34 can exist in more than two discrete forms (Htun & Dahlberg, 1989). The linked tip structures shown in Figure

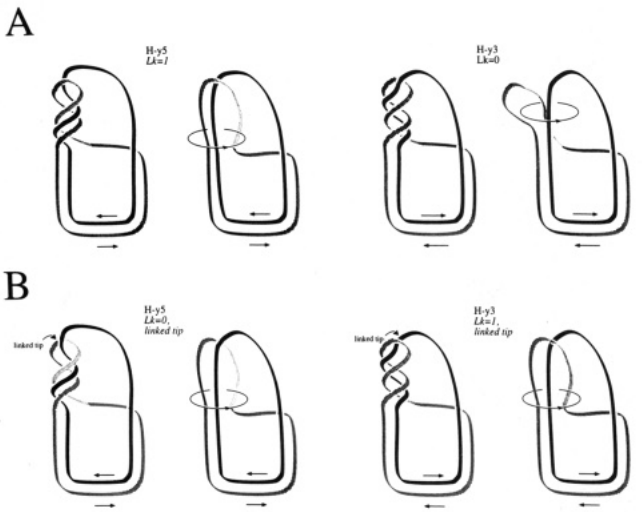

FIGURE 6: Topology of the isomeric forms of H DNA. Topological properties of the H-y5 and H-y3 forms are illustrated in closed circular models that contain either of the isomeric H forms (left-most structure in each pair). Unwrapping the polypyrimidine hairpin in the triplex (right-most model in every pair) reveals its linkage (Lk). The indicated direction of wrapping of the polypyrimidine hairpin reforms the triplex. Polypurine strands in the structures are indicated by solid lines, the portion of the polypyrimidine strand antiparallel to the polypurine strand by striped lines, and the portion of the polypyrimidine strand Hoogsteen paired and parallel to the polypurine strand by shaded lines. Straight arrows indicate strand polarity and point in the 5′ → 3′ direction. (A) H-y5 and H-y3 forms containing unlinked tip conformations topologically analogous to those in Figure 5. (B) H-y5 and H-y3 forms with linked tips (the purine strand passes through the pyrimidine hairpin).

6B are candidates for the additional forms since they cannot be interconverted without the tract first reverting to a nonprotonated duplex. However, linked tip structures may be disfavored over unlinked tips by hydrogen bond and stacking disruptions and electrostatic repulsions. The alternative proposal that the additional forms may be H-y3 or H-y5 forms differing in the length of triplex (Htun & Dahlberg, 1989) requires that there be distinct points in the apparently homogeneous tracts at which folding is permitted. This model requires that sliding of the strands, which would cause interconversion of the forms, must be effectively forbidden. Determination of the depurination patterns of these additional forms may assist in establishing their nature.

Several aspects of the family of folded "H DNA" $d(TC)_n$-$d(GA)_n$ structures have not yet been resolved. For example, the patterns of S1 nuclease sensitivity of the pyrimidine strands of $d(TC)_n$-$d(GA)_n$ H forms (Pulleyblank et al., 1985) now suggest that the triplex segments contain unusual backbone torsion angles not present in the classic triplex model (Arnott & Selsing, 1974). Such details of the H DNA model as the geometries of loop folding at the end of the triplex segment and of the multistrand junction at the base of the triplex have not yet been fully defined. It is not yet clear that strand disproportionation is a general requirement for protonation of DNA. Certain polypurine/polypyrimidine sequences such as the palindromic sequence $d([TC]_8A[GA]_8)$-$d([TC]_8T[GA]_8)$ (Glover et al., 1990) and the asymmetrical sequence $d(TTCTCC)_4$-$d(GGAGAA)_4$ (Farah and Pulleyblank, unpublished) undergo transitions to protonated states that do not exhibit characteristic markers of H DNA. Structural transitions induced by low pH have also been observed in a number of nonpolypurine/polypyrimidine sequences, including random sequences subject to external strain (Glover et al., 1988) and the telomeric sequence $d(GGGGTT)_n$-$d(AACCCC)_n$ (Lyamichev et al., 1989). These

transitions cannot easily be interpreted in terms of triplex formation.

References

Arnott, S., & Selsing, E. (1974) *J. Mol. Biol. 88*, 509–521.

Blommers, M. J. J., Walters, J. A. L. I., Haasnoot, C. A. G., Aelen, J. M. A., van der Marel, G. A., van Boom, J. H., & Hilbers, C. W. (1989) *Biochemistry 28*, 7491–7498.

Evans, T., & Efstratiadis, A. (1986) *J. Biol. Chem. 261*, 14771–14780.

Glover, J. N. M., & Pulleyblank, D. E. (1990) *J. Mol. Biol.* (in press).

Glover, J. N. M., Haniford, D. B., & Pulleyblank, D. E. (1988) *Nucleic Acids Res. 16*, 5473–5490.

Haasnoot, C. A. G., Hilbers, C. W., van der Marel, G. A., van Boom, J. H., Singh, U. C., Pattabiraman, N., & Kollman, P. A. (1986) in *Biomolecular Stereodynamics IV* (Sarma, R. H., & Sarma, M. H., Eds.) pp 101–116, Adenine Press, Schenectady, NY.

Haniford, D. B., & Pulleyblank, D. E. (1983) *Nature 302*, 632–634.

Hanvey, J. C., Klysik, J., & Wells, R. D. (1988a) *J. Biol. Chem. 263*, 7386–7396.

Hanvey, J. C., Shimizu, M., & Wells, R. D. (1988b) *Proc. Natl. Acad. Sci. U.S.A. 85*, 6292–6296.

Harvey, S. C., Luo, J. & Lavery, R. (1988) *Nucleic Acids Res. 16*, 11795–11809.

Htun, H., & Dahlberg, J. E. (1988) *Science 241*, 1791–1796.

Htun, H., & Dahlberg, J. E. (1989) *Science 243*, 1571–1576.

Htun, H., & Dahlberg, J. E. (1990) in *Structure and Methods: DNA & RNA* (Sarma, R. H., & Sarma, M. H., Eds.) Vol. 3, pp 185–206, Adenine Press, Schenectady, NY.

Iida, S., & Hayatsu, H. (1970) *Biochim. Biophys. Acta 213*, 1–13.

Izatt, R. M., Christensen, J. J., & Rytting, J. H. (1971) *Chem. Rev. 71*, 439–481.

Johnston, B. H. (1988) *Science 241*, 1800–1804.

Keller, W. (1975) *Proc. Natl. Acad. Sci. U.S.A. 72*, 4876–4880.

Kohwi, Y., & Kohwi-Shigematsu, T. (1988) *Proc. Natl. Acad. Sci. U.S.A. 85*, 3781–3785.

Lee, J. S., Johnson, D. A. & Morgan, A. R. (1979) *Nucleic Acids Res. 6*, 3073–3091.

Lee, J. S., Wordsworth, M. L., Latimer, L. J. P., & Morgan, A. R. (1984) *Nucleic Acids Res. 12*, 6603–6614.

Lyamichev, V. I., Mirkin, S. M., & Frank-Kamenetskii, M. D. (1985) *J. Biomol. Struct. Dyn. 3*, 327–338.

Lyamichev, V. I., Mirkin, S. M., & Frank-Kamenetskii, M. D. (1986) *J. Biomol. Struct. Dyn. 3*, 667–669.

Lyamichev, V. I., Mirkin, S. M., Danilevskaya, O. N., Voloshin, O. N., Balatskaya, S. V., Dobrynin, V. N., Filipov, S. A., & Frank-Kamenetskii, M. D. (1989) *Nature 339*, 634–637.

Lyamichev, V. I., Frank-Kamenetskii, M. D., & Soyfer, V. N. (1990) *Nature 344*, 568–570.

Mirkin, S. M., Lyamichev, V. I., Drushlyak, K. N., Dobrynin, V. N., Filippov, S. A., & Frank-Kamenetskii, M. D. (1987) *Nature 330*, 495–497.

Morgan, A. R., & Wells, R. D. (1968) *J. Mol. Biol. 37*, 63–80.

Pulleyblank, D. E. (1988) in *Nucleic Acids and Molecular Biology* (Eckstein, F., & Lilley, D. M. J., Eds.) Vol. 2, pp 31–48, Springer-Verlag, Berlin.

Pulleyblank, D. E., Haniford, D. B., & Morgan, A. R. (1985) *Cell 42*, 271–280.

Shapiro, R., & Danzig, M. (1972) *Biochemistry 11*, 23–29.

Voloshin, O. N., Mirkin, S. M., Lyamichev, V. I., Belotserkovskii, B. P., & Frank-Kamenetskii, M. D. (1988) *Nature 333*, 475–476.

Wells, R. D., Collier, D. A., Hanvey, J. C., Shimizu, M., & Wohlrab, F. (1988) *FASEB J. 2*, 2939–2949.

Zoltewicz, J. A., Clark, E. F., Sharpless, T. Q., & Grahe, G. (1970) *J. Am. Chem. Soc. 92*, 1741–1750.